A New Similarity Rule for Fluidized Bed Scale-up

A rule of hydrodynamic similarity for a scale change of fluidized beds has been developed based on the governing equations of bubble and interstitial gas dynamics. When geometrically similar scale-up is to be carried out maintaining hydrodynamic similarity, the proposed similarity rule requires that two conditions be satisfied. The first condition assures a similarity in bubble coalescence. The second assures the similarities in bubble splitting and in the interstitial flow pattern. The present work proves theoretically that these two conditions are the necessary, and almost sufficient, conditions for hydrodynamic similarity. They consider not only bubble coalescence but also bubble splitting. The theory proposed was first tested by previous correlations for bubble diameter and grid zone structure, and second by experiment. It has been proved that as long as the present rule is satisfied, the longitudinal distribution of the average bubble diameter, stochastic variation around it, and the radial distribution of superficial bubble velocity can be maintained similar for a scale change.

Application of the present rule to predict the bubbling and solid circulation characteristics in a large-scale unit by a small-scale experiment has thus proved promising, at least for Geldart group B particles. In order to further study the possibility of a similarity in mass transfer and chemical reactions, computation was carried out using the three-phase bubble assemblage model. If the effect of molecular diffusion is negligible, as in the case of fluidized bed combustion, even a chemical similarity is found to be possible.

Masayuki Horio and Akira Nonaka
Department of Applied Chemistry for Resources
Tokyo University of Agriculture and Technology
Koganei, Tokyo 184 Japan

Yoshitaka Sawa and Iwao Muchi
Department of Iron and Steel Engineering
Nagoya University
Nagoya, 464 Japan

SCOPE

Although fluidization has a number of advantages—such as temperature uniformity, good particle mixing, capability of continuous particle handling, adaptability to elevated temperatures and pressures, high heat transfer rate, and the possibility of sophisticated gas-solid system developments—a situation often arises where development is terminated or abandoned because of time shortage and/or remaining risks in the scale-up. Previous fluidization theory is lacking especially in the handling of the lateral distribution problem, which in many practical situations is much more important than other problems. The lateral bubble distribution is affected by column design, including such things as tapered walls, distributor structure and its nonuniformity, and internal baffles.

In the course of wide application of fluidization technology, reliable theories and corresponding techniques for experimental confirmation have been needed to handle the above-mentioned factors. Based on the Clift and Grace (1971) model for bubble coalescence, Horio et al. (1983a) developed a computer code for direct simulation of bubbling in a large-scale fluidized bed to predict its bubbling and solid circulation characteristics. However, the computation load of the direct simulation becomes heavier with increasing bed scale, while the result is not sufficiently persuasive for operating conditions far from those already experienced or seen in the literature.

The objective of the present paper is to propose a new methodology for solving the above-mentioned

problem. A new similarity rule based on the simulation model of Horio et al. (1983a), with modifications taking into account the effect of bubble splitting and the Davidson (1961) model for interstitial flow, is presented. Contrary to the conventional scale-up methodology based on the identity rule, which is unable to solve the problems relevant to the lateral flow patterns, the similarity rule in this paper reveals the need to examine the fluidization phenomena from the point of view of geometrical similarity. The present rule requires that for geometrically similar bubbling conditions, two conditions must be satisfied. It has been proven theoretically that these are the necessary, and almost sufficient, conditions. Because of the lack of data on the fluidizing behavior of group A particles in the Geldart (1973) classification, comparisons of the proposed theory with the data obtained in this study using group B particles is presented as the first step toward the complete validation of the theory. The theory has been successfully tested by both the previous correlations for bubble and jet sizes and the present data. The possibility and limitations of extending the present hydrodynamic similarity to the similarity in other rate processes are discussed with reference to the three-phase bubble assemblage model.

CONCLUSIONS AND SIGNIFICANCE

The Horio et al. (1983a) model for direct simulation of bubbling with modification to account for the effect of bubble splitting and the Davidson (1961) model for interstitial flow were used to develop a new scale-up methodology. It has been proved theoretically that the geometrical similarity in the hydrodynamics of the scale of bubbles can be established after a scale change of m times if, and almost only if, $u_0 - u_{mf} = \sqrt{m}\,(u_0 - u_{mf})^o$ and $u_{mf} = \sqrt{m}\,u^o_{mf}$, where superscript o denotes the values for the original scale unit. The first statement is the condition necessary for equivalent bubble coalescence. The second is the condition necessary for equivalent bubble splitting and similar interstitial flow pattern. This set of conditions is termed the similarity rule.

The theoretical prediction was first validated by previously proposed correlations for the cross-sectional averaged bubble diameter, the size of vertical and horizontal jets, and the solid dispersion. Secondly, the prediction was experimentally validated by three columns of 0.041, 0.10, and 0.24 m dia. The cross-sectional averaged bubble diameters, stochastic deviations around the average, and the radial distributions of superficial bubble velocities were all found to be in agreement. The present validation is restricted to group B particles, although there is the possibility that this similarity rule is valid even for group A particles.

To investigate the possibility of a similarity in chemical reaction, computation was carried out using the three-phase bubble assemblage model. It was found that such similarity is likely for beds of group B particles such as fluidized bed combustors. However, due to the high contribution of molecular diffusivity that does not vary in proportion to the intensity of convection, there seems to be little possibility of finding such a chemical similarity in fine catalyst beds.

The significance of the present results lies in the hydrodynamic similarity in the radial bubble distribution. Since the lateral bubble distribution controls the solid circulation, the present scale-up rule is expected to be applicable to optimization of particle feeding, circulation, and discharge, by changing the design of the column shape, internals, the distributor, and the location of feeders and downcomers. By using the similarity rule for the scale-down, the small-scale cold tests can be organized easily. The present rule is probably the first rigorous methodology for such design aspects. For scale-up and development problems it is suggested that both the present rule and the conventional identity rule be applied. The identity rule, which deals with the diameter increase only, is good for studying chemical reactions, while the present rule is good for testing the bubble distribution and solids handling.

Background

Among a number of gas-solid contacting modes the fluidization mode is most advantageous for processes involving a large contacting surface area per unit bed volume, uniformity of the state of particles, and the capability of continuous solid feeding or discharge even under pressurized conditions. The fluidization mode is also the most complicated, dynamic, and stochastic, not only in physical characteristics, but also in chemical reaction performance. Due to this complexity, scale-up methodology has so far been largely empirical and no general and systematic method has been established, although one has been intensively sought for decades.

The essential multiphase nature was pointed out early in the first period of fluidization study, which was initiated by Lewis and Gilliland in 1938 (Jahnig et al., 1980). Applying Kuhn's (1962) concept of paradigm (i.e., "universally recognized scientific achievements that for a time provide model problems and solutions to a community of practitioners"), the history of fluidization theory since Lewis and Gilliland can be divided into four periods through which we have been getting closer to a comprehensive scale-up methodology.

The most important concept resulting from the first period (i.e., up to the early 1950's) is the two-phase theory of Toomey and Johnstone (1952). This theory became the paradigm for the work of the second period (1953–1962), during which the structure of the bubble phase was investigated, first experimentally (Yasui and Johanson, 1958; Lanneau, 1960) and then theoretically, by Davidson (1961). From his hydrodynamic model for the flow field around a bubble Davidson predicted the presence of a cloud. This added another complex feature to the multiphase structure of fluidized beds. This prediction was confirmed experimentally by Rowe et al. (1962, 1964). The second period was closed with the revolutionary success of hydrodynamic modeling of fluidized particles. During the third period (1963–1973) fluidization theory was systematically organized based on bubble hydrodynamics. Most of the rate processes in the bed, including gas interchange between phases, heat transfer, solid circulation and dispersion, and reactor performances, were correlated in terms of bubble characteristics. Along with this systematization of the fluidized bed rate phenomena, efforts were directed toward the study of the fluidizing characteristics of different powders, of beds of different diameters, and of much higher gas velocities or pressures. At the end of the third period these efforts finally yielded three important results: a new understanding of the fluidized bed scale effect on radial flow distribution (Werther, 1973); a map for powder characterization (Geldart, 1973); and the rediscovery of a "highly expanded fluid bed" (Reh, 1971) that had first been studied by Lewis and Gilliland (1940) and was later named "fast fluidized bed" by Yerushalmi et al. (1976).

The fourth period dates from 1974. Since then the above findings have been working as a combined paradigm. Bubble diameter correlations have become more reliable during this period. Detailed investigations have been organized to understand comprehensively the modes of fluidization over a wide range of temperature, pressure, particle size, fluidizing velocity, and column diameter. Much attention has also been paid to the boundary regions such as the grid zone, the freeboard, and the stand pipes. However, most of the correlations presented so far are restricted to certain ranges of powder type, particle size, column size, gas velocity, pressure, and temperature. These limitations in the previous correlations reduce the reliability of the predicted values for commercial-scale plants. They also make it difficult to obtain useful information sufficiently from small-scale models and cold models. Therefore, the scale-up of fluidized bed reactors so far has had to be done in an empirical manner, introducing many stages between laboratory-scale units and the final commercial plants.

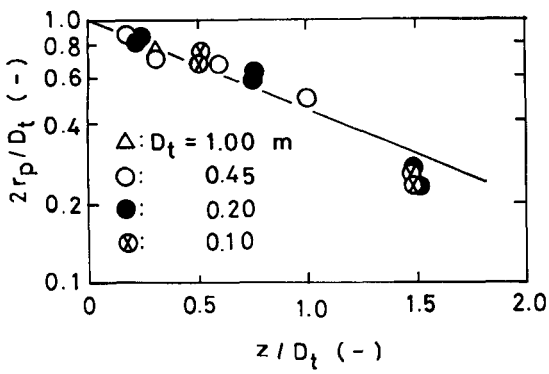

Figure 1. Radial location of maximum bubble flow vs. height.

In the ordinary scale-up methodology it is a fundamental rule that the same particle, the same bed height, and the same gas velocity must be used. Distributor parameters, including the fraction of open area, cap or tube size, and orifice diameter and pitch also have to be kept constant. As long as this rule is satisfied an approximate identity of the longitudinal distribution of bubble parameters, such as the average bubble diameter and bubble fraction, can be made and thus the chemical reactions can be expected to be identical. The increase in the capacity of the system is mainly given by the increase in the cross-sectional area. In this paper this is called the identity rule.

The essential disadvantages of the identity rule are:

1. The scaling-down of commercial concepts to laboratory units is limited because of the onset of slugging below a certain bed diameter.

2. No information can be gathered from smaller scale models because bubble distribution changes considerably with bed diameter.

3. The phenomena related to particle circulation pattern, which is much affected by the radial bubble distribution, cannot be tested by smaller models.

4. The effects of the global structure of the bed, including column shape, stand pipe, feeder, and internals and/or distributor designs, are difficult to predict from small-scale experiments.

The objective of this paper is not to propose a completely new scale-up method, but to present a new similarity rule that, combined with the above-mentioned identity rule, will reinforce the theoretical background for scale-up technology. This similarity rule provides the criteria for establishing a geometrical similarity of fluidized bed performance between models of different sizes but of the same geometrical structure. To attain a geometrically similar fluidizing condition between beds of different scales, this similarity rule requires that both fluidizing gas velocity and minimum fluidization velocity be varied proportionally with the square root of the scale ratio. This means that the similarity rule does not require a geometrical similarity for particles.

Looking back to the past, anticipation of the present similarity rule can be found in previously published data. Figure 1 shows the Werther (1973) data replotted by Mori and Wen (1975). It can be seen that the maximum of the superficial bubble velocity appears at the same relative location in the bed. Strictly speaking, the requirements of the similarity rule are not satisfied in the case of the Werther experiment, because the same porous plate and the same gas velocity were used for every run. However, Figure 1 is still very interesting for it suggests the presence of a certain geometrical similarity. During the recent progress of fluidized bed combustor development the need for a rational scale-up methodology has again been strongly recognized. Fitzgerald et al. (1983, 1984) presented a consideration based on the Reynolds number and Froude number analogies taking the particle size as the representative length. The grounds for this consideration, however, were not rigorously established. Horio et al. (1982) presented preliminary results of hydrodynamic consideration and experimentation to establish a new similarity rule.

The necessary and almost sufficient conditions for a geomet-

rical similarity of fluidization are derived theoretically in this paper. To validate the present similarity rule, previous bubble correlations are reviewed to examine if they are consistent with the present conditions and the authors' experimental validation is presented. Application of the rule for scale-up and reactor development is also discussed.

Theory

Formulation of bubbling fluidized beds

The hydrodynamic structure of a fluidized bed is determined as the solution of a set of equations for gas and solid motion such as the Anderson-Jackson (1967) model subject to the boundary conditions for the particular geometry and operating conditions of the bed. Garg and Pritchett (1975) demonstrated, after extremely laborious computation, that jets and bubbles can be obtained as a numerical solution of such equations. However, it is difficult to apply such fundamental equations to the analytical consideration of bubbling bed behavior, because they do not explicitly express bubbles. To avoid mathematical complexities of such strict treatment the present work is founded on a direct simulation model for bubble motion, i.e., a modified version of the Horio et al. (1983a) model. The basic assumptions for the present formulation are:

1. The particle phase is well fluidized and the gas flow allotment to the bubble phase and the emulsion phase is approximately expressed by the two-phase theory of Toomey and Johnstone (1952).
2. The flow of particles and the flow of interstitial gas are described by the Davidson (1961) equations.
3. The interaction of bubbles in a swarm can be expressed by the superposition of the interaction between two bubbles isolated from others; the latter can be estimated by the Clift and Grace (1971) model, which is derived from the potential flow assumption for particle flow.
4. The bubble splitting process can be expressed by the Horio and Nonaka (1984) model where the splitting frequency of a single bubble is assumed to be proportional to $u_{mf}^{-1.2}$, based on the data of Toei et al. (1974).

Assumption 1 is valid for most of the group B particles of Geldart's classification. It is also valid for the cases in which the gas velocity is much higher than the minimum fluidizing velocity, regardless of the powder type. Assumption 2 may be replaced by the Murray (1965) model, but the difference is not a major one. The measurement of gas velocity by hot wire anemometry (Nguyen et al., 1976) has shown that the Davidson model is still in agreement with the observed velocity. In regard to assumption 3, Clift and Grace proposed their coalescence model for two isolated bubbles already with experimental validation. The superposition of the model in the cases of freely bubbling conditions was tried and confirmed by Horio et al. (1983a). They confirmed that satisfactory bubble simulation is possible with a slight modification of the bubble velocity coefficient. Although some more investigation is required, the validity of assumption 4 has been confirmed over the range of $D_t = 0.079 \sim 1.0$ m, $u_0 = 0.05 \sim 0.5$ m/s, and $u_{mf} = 1.6 \times 10^{-3} \sim 0.1$ m/s (Horio and Nonaka, 1984). Thus, combining the above four assumptions, a considerably general model of the fluidization phenomena can be constructed.

To define the time-averaged characteristics of a fluidized bed by any model, two local time-averaged parameters, the bubble fraction and the bubble diameter, are necessary and sufficient. The local time-averaged bubble fraction ϵ_b is given by

$$\epsilon_b = \frac{u_{b0}}{u_b}. \tag{1}$$

where u_{b0} is the local superficial bubble velocity, i.e., the local visible bubble flow rate per unit cross-sectional area of bed, and u_b is the local time-averaged bubble rising velocity.

Integration of $u_b\epsilon_b$ over the cross section with assumption 1 yields

$$\bar{\epsilon}_b = \frac{u_0 - u_{mf}}{\bar{u}_b}, \tag{2}$$

where $\bar{\epsilon}_b$ and $\bar{u}_b$ are the cross-sectional averages of bubble fraction and bubble rising velocity, respectively.

In regard to both the local time-averaged superficial bubble velocity u_{b0} and the local time-averaged bubble diameter, no method has been established to predict them directly by solving certain governing equations. The only method available at present is first to solve the equation of motion for each bubble taking into account the bubble coalescence, and then to calculate the time average variables from the bubble trajectory data. Horio et al. (1983a) presented a method by which one can simulate lateral bubble distributions and solid circulation patterns in large scale fluidized beds. The major equations in their model are as follows.

Location and diameter of an arbitrary bubble i

$$\frac{dx_{bi}}{dt} = u_{bi} \quad (\forall i \in B) \tag{3}$$

$$D_{bi} = \left[D_{b0}^3 + \sum_{j \in B_i'} D_{bj}^3 \right]^{1/3}, \tag{4}$$

where B is the set of existing bubbles in the bed, and B_i' is the set of bubbles already absorbed by the bubble i. The computation for the bubbles absorbed by the bubble i is, of course, terminated at the time of coalescence.

Initial condition for the integration

$$D_{bi} = D_{b0} \quad \text{and} \quad x_{bi} = x_{0i} \quad \text{at } t = t_i. \tag{5}$$

From the Davidson and Harrison (1963) model

$$t_i = t_{i-1} + D_{b0}^3/[(u_0 - u_{mf})A_t] \tag{6}$$

$$D_{b0} = 1.3g^{-0.2}[(A_t/n_n)(u_0 - u_{mf})]^{0.4}. \tag{7}$$

In the simulation by Horio et al. (1983a) a random variable of uniform distribution was used to determine the initial timing of bubble formation from each orifice. In order to express the fluctuation around the mean period of bubble formation from each orifice a random variable of normal distribution was applied.

Rising velocity of bubble i in a freely bubbling bed

$$\boldsymbol{u}_{bi} = u_{b\infty i}\boldsymbol{e}_z + \sum_{\substack{j\in B \\ j\neq i}} \Delta\boldsymbol{u}_{ij}, \tag{8}$$

where

$$u_{b\infty} = \xi k_{b\infty}\sqrt{gD_b}. \tag{9}$$

Horio et al. (1983a) adjusted the parameter ξ by

$$\xi = \begin{cases} 0.6 & [u_{b0}/(u_0 - u_{mf})] > 0.6 \quad (10a) \\ u_{b0}/(u_0 - u_{mf}) & [u_{b0}/(u_0 - u_{mf})] < 0.6 \quad (10b) \end{cases}$$

so that the computed results correspond with the Whitehead and Young (1967) data and with the GOLFERS (1982) data. Δu_{ij}, the increment of velocity of the bubble i due to the interaction with the bubble j, is a function of the size of the two interacting bubbles and their relative location. That is

$$\Delta\boldsymbol{u}_{ij} = u_{b\infty j}\boldsymbol{F}_{ij}(s, z_d^+, r_d^+, b), \tag{11}$$

where

$$s = D'_{bi}/D'_{bj} \tag{12}$$

$$z_d^+ \equiv (z_{bj} - z_{bi})/R'_{bj} \tag{13}$$

$$r_d^+ \equiv [(x_{bj} - x_{bi})^2 + (y_{bj} - y_{bi})^2]^{1/2}/R'_{bj} \tag{14}$$

$$b \equiv \tan^{-1}\frac{y_{bj} - y_{bi}}{x_{bj} - x_{bi}}. \tag{15}$$

The details of the function $\boldsymbol{F}$ in Eq. 11 are not present here but can be found in the Clift and Grace (1971) paper. The significant feature of $\boldsymbol{F}$, however, is that its value is conserved during a geometrically similar scale change.

Such simulation becomes more realistic if bubble splitting is also taken into account. Horio and Nonaka (1984) tentatively correlated the splitting frequency for a single bubble in the course of its rising by

$$f_s^* = 6.5 \times 10^{-3} u_{mf}^{-1.2}. \tag{16}$$

Now, to rewrite the set of the above equations into dimensionless forms the following dimensionless parameters are introduced:

$$D_b^+ = D_b/D_t, \quad f_s^{*+} = f_s^*\sqrt{D_t/g},$$
$$t^+ = t\sqrt{g/D_t}, \quad u_{bi}^+ = u_{bi}/\sqrt{gD_t},$$
$$x_{bi}^+ = x_{bi}/D_t,$$

where D_t is adopted as the representative length. Since in the present model the height of the bed surface has no special effect, and since the particle size is not included in the model explicitly, D_t is the only length parameter corresponding to the operating conditions. In regard to the particle diameter, it should not be used as the representative length because it is a parameter for the microscopic interstitial flow field. In other words, the particle phase has to be treated as a continuous phase to focus our attention on the macroscopic flow field in the bed.

Then, we have

$$\frac{dx_{bi}^+}{dt^+} = \boldsymbol{u}_{bi}^+ \tag{17}$$

$$D_{bi}^+ = \left[D_{b0}^{+3} + \sum_{j\in B'_i} D_{bj}^{+3}\right]^{1/3} \tag{18}$$

$$\boldsymbol{u}_{bi}^+ = \xi k_{b\infty}\left[\sqrt{D_{bi}^+}\,\boldsymbol{e}_z + \sum_{\substack{j\in B \\ j\neq i}} \sqrt{D_{bj}^+}\,\boldsymbol{F}_{ij}\right] \tag{19}$$

$$D_{bi}^+ = D_{b0}^+ \quad \text{and} \quad x_{bi}^+ = x_{0i}^+ \quad \text{at } t^+ = t_i^+ \tag{20}$$

$$D_{b0}^+ = 1.3[(\pi/4n_n)(u_0 - u_{mf})/\sqrt{gD_t}]^{0.4} \tag{21}$$

$$t_i^+ = t_{i-1}^+ + (4/\pi)[D_{b0}^{+3}\sqrt{gD_t}/(u_0 - u_{mf})] \tag{22}$$

$$f_s^{*+} = \frac{6.5 \times 10^{-3}}{g^{1.1}D_t^{0.1}}\left(\frac{u_{mf}^2}{gD_t}\right)^{-0.6}. \tag{23}$$

If the transient version of the Davidson differential equations were solved subject to the bubble motion obtained from Eqs. 17 to 23, the gas and particle flow in the vicinity of bubbles could be determined. However, the mathematical expression for the conditions at the bubble boundary for such a situation is too complicated for our present concern. Since our purpose is to find the parameters controlling the flow around bubbles, we will not lose the generality even if we assume that the gas and particle flow fields in the vicinity of a bubble are approximately equal to those around an isolated single bubble. Then, from Davidson (1961) we have the following dimensionless stream function of interstitial gas and the dimensionless velocity potential for dense phase particles:

$$\psi_f^+ = \frac{u_{emf}}{\sqrt{gD_t}}\left[\alpha_b - 1 + (\alpha_b + 2)\frac{R_b^{+3}}{r^{+3}}\right]\frac{r^{+2}\sin^2\theta}{2} \tag{24}$$

$$\Phi_s^+ = -\frac{u_{b\infty}}{\sqrt{gD_t}}\left[r^+ + \frac{R_b^{+3}}{2r^{+2}}\right]\cos\theta, \tag{25}$$

where

$$\alpha_b \equiv \frac{u_{b\infty}}{u_{emf}} \tag{26}$$

and

$$u_{emf} = \frac{u_{mf}}{\epsilon_{mf}}. \tag{27}$$

R_b^+ is the dimensionless bubble radius, r^+ is the dimensionless distance from the bubble center, and θ is the angle from the vertical axis.

When $\alpha_b > 1$ a cloud is formed around a bubble. The dimensionless cloud radius R_c^+ is given by

$$\left(\frac{R_c^+}{R_b^+}\right)^3 = \frac{\alpha_b + 2}{\alpha_b - 1}, \tag{28}$$

Derivation of the similarity rule

Based on the above description of the fluidized conditions a rule for a complete geometrical similarity is derived. As shown in Figure 2, the fluidizing condition in a geometrically similar model m times larger than the base model is considered. Here it is assumed that the bed height, column diameter, distributer orifice diameter, orifice pitch, and other structural parameters are changed in the same proportionality such as

$$m = \frac{L_f}{L_f^o} = \frac{D_t}{D_t^o} = \frac{P_n}{P_n^o} = \frac{d_n}{d_n^o}, \tag{29}$$

where the superscript o denotes the base condition.

Since the hydrodynamic condition of a fluidized bed is almost completely determined by the bubble behavior, having a geometrically similar fluidizing condition between the above-described two beds is equivalent to having a geometrically similar bubbling condition between them. Thus, if the following conditions are satisfied, both fluidized beds are expected to show equivalent hydrodynamical behaviors:

Condition for identical bubble fraction

$$\epsilon_b(x^+, y^+, z^+) = \epsilon_b^o(x^+, y^+, z^+), \tag{30a}$$

where (x^+, y^+, z^+) are the dimensionless Cartesian coordinates, z^+ for vertical axis. Taking the average of Eq. 30a over the cross section, we have

$$\bar{\epsilon}_b = \bar{\epsilon}_b^o. \tag{30b}$$

Condition for a geometrically similar bubble size distribution

$$\frac{D_b(x^+, y^+, z^+)}{D_b^o(x^+, y^+, z^+)} = m. \tag{31}$$

Condition for equivalent splitting frequency

$$f_s^{*+} = f_s^{*+o} \tag{32}$$

Condition for geometrical similarity of the flow field around each bubble

$$\frac{u_e(r^+, \theta)}{u_{b\infty}(D_b)} = \frac{u_e^o(r^+, \theta)}{u_{b\infty}(D_b^o)}, \tag{33}$$

$$\frac{v(r^+, \theta)}{u_{b\infty}(D_b)} = \frac{v^o(r^+, \theta)}{u_{b\infty}(D_b^o)}, \tag{34}$$

where (r^+, θ) are the dimensionless polar coordinates locating its origin on the bubble center, and u_e and v are the gas and solid velocities in the emulsion phase, respectively. Their radial and tangential components are given by

$$u_{er}^+ = -\frac{1}{r^{+2} \sin\theta} \frac{\partial \psi_f^+}{\partial \theta}, \tag{35}$$

$$u_{e\theta}^+ = \frac{1}{r^+ \sin\theta} \frac{\partial \psi_f^+}{\partial r^+}, \tag{36}$$

$$v_r^+ = \frac{\partial \Phi_s^+}{\partial r^+}, \tag{37}$$

$$v_\theta^+ = \frac{1}{r^+} \frac{\partial \Phi_s^+}{\partial \theta}. \tag{38}$$

Here, the fundamental equations, Eqs. 17 to 25, introduced above are examined relevant to the scale change effect. In the present formulation those parameters having length in their

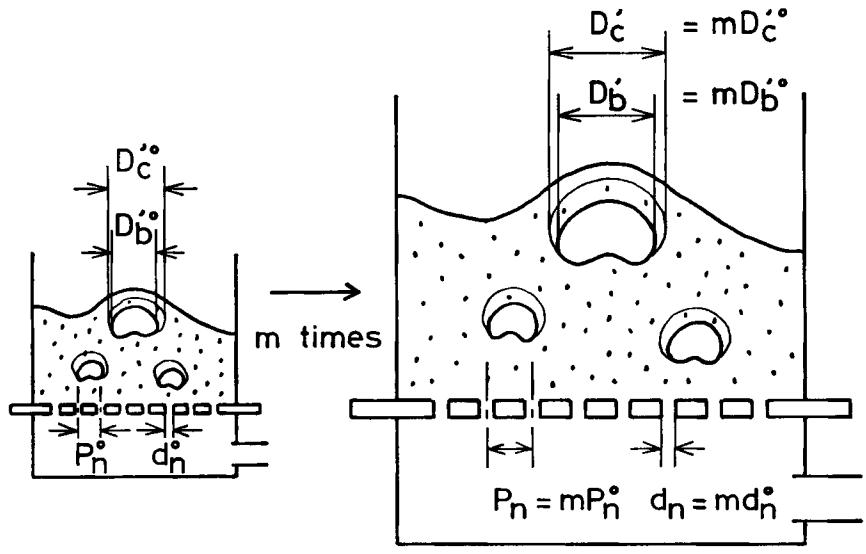

Figure 2. Two beds of complete geometrical similarity.

dimensions are made into dimensionless form by adopting not the particle size but the column diameter D_t as the representative length. Therefore, if the dimensionless equations remain invariant through the change in bed scale, the results for local time-averaged values such as dimensionless bubble size and bubble fraction also remain invariant. This is the case where a geometrical similarity is attained.

In the present model the equations having D_t as their parameters are Eqs. 21 to 25. Equations 21 and 22 are to be invariant during the scale change if, and only if,

$$\frac{u_0 - u_{mf}}{\sqrt{gD_t}} = \frac{(u_0 - u_{mf})^o}{\sqrt{gD_t^o}}. \tag{39}$$

On the other hand, Eqs. 24 and 25 are invariant if, and only if,

$$\frac{u_{mf}}{\sqrt{gD_t}} = \frac{u_{mf}^o}{\sqrt{gD_t^o}}. \tag{40}$$

The above relation also makes Eq. 23 almost invariant. In the denominator of Eq. 23 the part $(gD_t)^{0.1}$ is not nullified by the nondimensionalization, although the effect is almost negligible. At present, however, no solution to this problem seems to be imminent, because whether the power in correlation 16 is 1.2 or 1.0 is still open to future investigation due to the lack of sufficient experimental data. Rearranging Eqs. 39 and 40, we have the final expression for the necessary and almost sufficient conditions:

Condition for geometrically similar bubble coalescence

$$u_0 - u_{mf} = \sqrt{m}(u_0 - u_{mf})^o. \tag{41}$$

Condition for a geometrically similar flow field around a bubble and for similar bubble splitting

$$u_{mf} = \sqrt{m}\, u_{mf}^o. \tag{42}$$

For group B powders where splitting is negligible, the first condition is sufficient for geometrically similar distribution of bubble diameter and bubble fraction.

Therefore, if any information is needed about the fluidizing condition of a commercial-scale plant to be developed, the following procedure can be used to predict it. First, a complete $1/m$ scale model, including the distributor structure, is constructed and particles whose u_{mf} is $1/\sqrt{m}$ of that of the particles to be used in the commercial scale operation are charged into the column. The bed height is also adjusted in the same proportion. Then, if the bed is fluidized by gas with a velocity of $1/\sqrt{m}$ times the base condition, geometrically similar bubbling is established. The requirements of the second condition assure the similarity of the hydrodynamic condition of the dense phase.

It should be noted here that the above two simple conditions are proved to be not only necessary conditions, but also sufficient conditions for attaining geometrically similar fluidizing conditions. The proof of sufficiency is complete for the first condition, but it is not for the second, because the present consideration for the flow field is restricted to the isolated single bubble. However, if the Davidson equations are solved for the boundary condition of a multibubble situation, the additional parameters are the bubble diameters and their locations. Thus the system remains more or less in a similar structure. Therefore, from such a general treatment of the problem the same results as Eq. 42 would be obtained.

The result that the condition of Eq. 41 is necessary can easily be derived without introducing Eqs. 17 to 22. That is, from Eqs. 2, 30, and 31 condition 41 is immediately obtained. The reason a rather complicated procedure has been taken here is to prove that the condition is a sufficient condition for the similarity not only for longitudinal distribution but also for radial distribution. The similarity in the radial bubble distribution is very important, because with this condition a geometrically similar radial solid circulation pattern may be obtained.

Validation of the Similarity Rule by Previous Correlations

Before testing the above similarity rule directly by experiments the consistency between the present rule and the previously proposed correlations for bubble diameter, particle diffusivity, and grid zone parameters are examined.

Longitudinal distribution of cross-sectional average bubble diameter

Only those correlations including the initial bubble diameter or a corresponding term are examined to see if they satisfy the present similarity rule. Here it is supposed that the bed is scaled up m-fold geometrically and that the particle size and the fluidizing gas velocity are changed according to the requirements of Eqs. 41 and 42. Then, if the bubble diameter from a correlation changes m times, the correlation is consistent with the similarity rule. The result of this test is shown in Table 1. It is interesting that although the mathematical structure of correlations by Chiba et al. (1973), Hirama et al. (1975), Mori and Wen (1975), Rowe (1976), and Darton et al. (1977) differ considerably, they all satisfy the present rule. Other correlations by Geldart (1971) and by Fryer (1974) screened out by the similarity rule may be limited in their applicability within a narrow range.

Slug behavior and onset of slugging

The rise velocity of a round-nosed slug is expressed by the following Stewart and Davidson (1967) correlation:

$$\frac{u_s}{\sqrt{gD_t}} = \frac{u_0 - u_{mf}}{\sqrt{gD_t}} + 0.35. \tag{43}$$

For the onset of slugging Stewart and Davidson presented the following criterion:

$$\frac{u_0 - u_{mf}}{\sqrt{gD_t}} = 0.07. \tag{44}$$

As far as these correlations are concerned, the behavior of slugs and the onset condition of slugging are consistent with the present similarity rule, since, from the condition in Eq. 39, both the righthand side of Eq. 43 and the lefthand side of Eq. 44 remain constant during the scale change based on the present similarity rule.

For square-nosed slugs the onset condition does not depend upon gas velocity. Yagi et al. (1952) presented the following

Table 1. Consistency of Previous Bubble Diameter Correlations with Present Similarity Rule

Investigator	Bubble Dia. Correlation	D_b/D_b^o	Consistency
Geldart (1971)	$D_b = D_{b0} + 0.27z(u_0 - u_{mf})^{0.94}$	$\dfrac{D_{b0} + 0.27z(u_0 - u_{mf})^{0.94}}{D_{b0}^o + 0.27z^o(u_0^o - u_{mf}^o)^{0.94}} = m \sim m^{1.47}$	No due to the nonlinear term $z(u_0 - u_{mf})^{0.94}$
Chiba et al. (1973)	$D_b = [1.245(z - z_{b0})/D'_{b0} + 1]^{2/7} D'_{b0}$, $z < z_k$ $D_b = \left[\dfrac{1.828(z - z_k)}{2^{(5k+1)/6} D_{bk}} + 1\right]^{2/3} D_{bk}$, $z > z_k$ $k \equiv \ln[(2P_n/D_{b0})/(1 + f_w)]/\ln 2$ $z_k \equiv z_{b0} + (2^{7k/6} - 1)D'_{b0}/1.245$ $D_{bk} \equiv 2^{k/3} D'_{b0}$, $h_{b0} \equiv h_j + 6D'_{b0}/7$	$\left[\dfrac{1.245(z - z_{b0})/D'_{b0} + 1}{1.245(z^o - z_{b0}^o)/D_{b0}^{\prime o} + 1}\right]^{2/7} \left(\dfrac{D'_{b0}}{D_{b0}^{\prime o}}\right) = m$ $\left[\dfrac{\dfrac{1.828(z - z_k)}{2^{(5k+1)/6} D_{bk}} + 1}{\dfrac{1.828(z^o - z_k^o)}{2^{(5k+1)/6} D_{bk}^o} + 1}\right]^{2/3} \left(\dfrac{D_{bk}}{D_{bk}^o}\right) = m$	Yes
Fryer (1974)	$D_b = D_{b0} + 2.05 \times 10^{-2} u_0 z$	$\dfrac{D_{b0} + 2.05 \times 10^{-2} u_0 z}{D_{b0}^o + 2.05 \times 10^{-2} u_0^o z^o} = m \sim m^{1.5}$	No due to the nonlinear term $u_0 z$
Hirama et al. (1975)	$D_b = \dfrac{1.1(u_0 - u_{mf})^{0.6} z^{0.6} D_t^{0.1}}{k_b^{0.67} g^{0.3}}$	$\left(\dfrac{u_0 - u_{mf}}{u_0^o - u_{mf}^o}\right)^{0.6} \left(\dfrac{z}{z^o}\right)^{0.6} \left(\dfrac{D_t}{D_t^o}\right)^{0.1} = m$	Yes
Mori and Wen (1975)	$\dfrac{D_{bm} - D_b}{D_{bm} - D_{b0}} = \exp(-0.3z/D_t)$	$\dfrac{D_{bm} + (D_{b0} - D_{bm}) \exp(-0.3z/D_t)}{D_{bm}^o + (D_{b0}^o - D_{bm}^o) \exp(-0.3z^o/D_t^o)} = m$	Yes
Rowe (1976)	$D_b = \dfrac{(u_0 - u_{mf})^{0.5}(z + z_{b0})^{0.75}}{g^{0.25}}$	$\left(\dfrac{u_0 - u_{mf}}{u_0^o - u_{mf}^o}\right)^{0.5} \left(\dfrac{z + z_{b0}}{z^o + z_{b0}^o}\right)^{0.75} = m$	Yes
Darton et al. (1977)	$D_b = \dfrac{0.54(u_0 - u_{mf})^{0.4}(z + 2\sqrt{\pi/n_n} D_t)^{0.8}}{g^{0.2}}$	$\left(\dfrac{u_0 - u_{mf}}{u_0^o - u_{mf}^o}\right)^{0.4} \left(\dfrac{z + 2\sqrt{\pi/n_n} D_t}{z^o + 2\sqrt{\pi/n_n} D_t^o}\right)^{0.8} = m$	Yes

onset criterion for square-nosed slugging:

$$L_{mf}/D_t = 1.9/(d_p \rho_p)^{0.3}. \tag{45}$$

For small particles of $Ar < 1.9 \times 10^4$, the critical L_{mf}/D_t changes with $m^{0.075}$ and the present similarity rule stands approximately because the change in d_p required by Eq. 42 is proportional to $m^{0.25}$. For large particles of $Ar > 2.45 \times 10^7$ the required change in d_p is proportional to m. This means that the particle size is changed similarly and the critical L_{mf}/D_t changes with $m^{-0.3}$; that may not be negligible in a scale change of large magnification. However when the same particles are used, the criterion (Eq. 45) is consistent with the present geometric similarity rule, although the similarity of the interstitial flow field is sacrificed.

Slugging phenomena are dependent on the distribution of powder stress in the bed, and therefore on the powder properties that may not be able to satisfy the present similarity rule. Baeyens and Geldart (1974) modified Eq. 44 by including a term to express the effect of bed height, which contradicts the present similarity rule. The empirically determined criterion by Broadhurst and Becker (1975) does not satisfy the present rule. These suggest that more work should be done to make any more detailed argument.

Particle circulation and dispersion

The rate of axial particle circulation induced by wake lifting and by drift motion is proportional to $u_0 - u_{mf}$ as written in the following:

$$q_s = (u_0 - u_{mf})A_t(f_w + f_d), \tag{46}$$

where f_w is the wake fraction, and f_d represents the contribution of drift motion. The relative intensity of axial circulation $q_s/[(u_0 - u_{mf})A_t]$ remains constant during the scale change. For the case where particle circulation is controlled by a buoyant effect, not by wake lifting, as in the case of a bubble column, the following expression is presented by Miyauchi et al. (1981):

$$v = 6\bar{\epsilon}_b v_0 \{e_b^2 + [1 - (r/R_t)^2]^2\} \tag{47}$$

where

$$e_b = [(2 - 3\bar{\epsilon}_b)/6(1 - \bar{\epsilon}_b)]^{1/2} \tag{48}$$

$$v_0 = gD_t^2/192\nu_t. \tag{49}$$

The turbulent kinematic viscosity ν_t is given by

$$\nu_t = 0.079(u_0 - u_{mf})^{1/6} D_t^{1.7}. \tag{50}$$

Substituting the similarity conditions into the above equations, the change of the relative circulation intensity $v/(u_0 - u_{mf})$ with the scale change of m times can be calculated. The result

is

$$\frac{[v/(u_0 - u_{mf})]}{[v/(u_0 - u_{mf})]^o} = m^{-0.283}, \tag{51}$$

where the power of m in the above equation should be zero if the similarity rule stands. Therefore, if the particle fluidity is as high as that of fine catalyst particles, there is a possibility that the circulation intensity deviates from the similarity condition to the extent given by Eq. 51.

In regard to the radial particle dispersion Kunii and Levenspiel (1969) applied the random walk model and presented the following relationship:

$$D_{sr} = \frac{3}{16}\frac{\epsilon_b}{1-\epsilon_b}\frac{u_{mf}D_b}{\epsilon_{mf}}. \tag{52}$$

Actually, the particle motion is induced by bubble motion and its representative velocity is u_b. Hirama et al. (1975) replaced u_{mf}/ϵ_{mf} in the above relation by u_b and proposed the following correlation:

$$Pe_s \equiv \frac{(u_0 - u_{mf})L_{mf}}{D_{sr}} = \frac{6.2}{f_w}\left[\frac{(u_0 - u_{mf})}{\sqrt{gD_t'}}\right]^{0.1}\left(\frac{L_{mf}}{D_t'}\right)^{0.5}, \tag{53}$$

where Dt' denotes the thickness of a two-dimensional bed or the diameter of a cylindrical bed. Using condition 41 the invariancy of the Peclet number during the scale change can easily be checked.

Grid zone structure

Approximately four to five parameters, i.e., initial bubble diameter, jet diameter, jet height, jet length for horizontal jetting, and dead zone height are essential for describing the hydrodynamic structure of a grid zone. Using Eq. 21 it has already been proved that the initial bubble diameter changes proportionally with the bed dimension if condition 41 is satisfied.

For jet diameter and height the consistency of the previously proposed correlations and the present similarity rule was examined. Results are summarized in Tables 2 and 3. It can be concluded from these tables that most of the correlations having certain theoretical background are almost consistent with the present rule, although the latter has been derived only from the analysis of bubbling characteristics. The reason for this consistency seems to be that the jetting phenomena is controlled by u_{mf} in the dense phase and by the kinematic energy $\rho_f u_n^2/2$ in the jet phase, both of which are automatically adjusted by Eqs. 41 and 42 during the scale change with geometrically similar bubbling.

For horizontal jetting Horio et al. (1983b) proposed the following semitheoretical correlation:

$$l_j/d_n = \xi_0 + \xi_1(d_n/d_p)^{0.2}(\rho_p/\rho_f)^{0.2}Fr_n^{0.4}, \tag{54}$$

where ξ_1 and ξ_2 are functions of u_0/u_{mf}. From Eqs. 29, 41, and 42 the change of jet length with the scale change of m times is given as follows:

$$\frac{l_j}{l_j^o} = m\left[\left(1 - \frac{\xi_0^o d_n^o}{l_j^o}\right)m^{0.15} + \frac{\xi_0^o d_n^o}{l_j^o}\right]. \tag{55}$$

In most cases the value $\xi_0^o d_n^o/l_j^o$ is much smaller than unity and the righthand side of Eq. 55 is nearly equal to $m^{1.15}$. It is understood that for a scale change within five times that of the original, the horizontal jet remains almost similar because the dimensionless jet length increases 27%; that is within the prediction error. Otherwise, the correlation may be applied to obtain the nozzle diameter d_n for an exactly similar jet length.

Concerning the dead zone on the perforated plate, Horio et al. (1980a) correlated the results by

$$\frac{h_s}{P_n} = \frac{\tan\phi_r}{2}\left(1 - \frac{d_m}{P_n}\right), \tag{56}$$

where d_m denotes the particle moving zone diameter around the orifice. Since the minimum value of d_m is d_n, the maximum value of h_s depends only on the angle of repose ϕ_r and $P_n - d_n$. Therefore, the maximum value of the dead zone height for noncohesive particles also remains similar.

As shown above, most of the parameters necessary to define the fluidized bed conditions seem to behave similarly during the scale change with the present similarity rule. It should be noted here that purely empirical correlations with no theoretical background tend not to satisfy the present similarity rule.

Experimental

Fluidized beds and bed materials

In order to validate the similarity rule derived above an experiment was carried out with three fluidized beds of different diameters but having completely similar geometry. The column diameters were 0.24 , 0.10, and 0.041 m. The columns were made of PMMA resin. Each bed was equipped with a similar perforated plate distributor with 223 holes drilled in a triangular arrangement. The particles used in the experiment are listed in Table 4. All powders belonged to group B of the Geldart (1973) classification. The beds were fluidized by ambient air.

Fluidizing conditions

The present experimental runs have been grouped into three series. In each run the longitudinal distribution of the cross-sectional average bubble diameter, the cumulative bubble diameter distribution in the bed cross section, and the radial distribution of superficial bubble velocity were measured. The conditions of the series A runs are shown in Table 5. The objective of this series was to examine whether the above three factors remain similar when both conditions 41 and 42 are satisfied. That is, both u_{mf} and $(u_0 - u_{mf})$ were changed $\sqrt{m}$ times so that both bubble and cloud diameters changed in a complete proportionality.

In test series B the same powder was used in every run, as listed in Table 6. In this case the exact equivalence of the cloud diameter is not established. However, such cases may often arise in the practical situations where it is impossible to change the particles.

Test series C was programmed to check whether the three powders show similar bubbling characteristics fluidized in the

Table 2. Consistency of Previous Jet Diameter Correlations with Present Similarity Rule

Investigator	Correlation	d_j/d_j^o	Consistency
Malek et al. (1963)	$d_j = (0.115 \log P_n - 0.031)G^{0.5}$ $G = A_t(u_0 - u_{mf})/n_n$	$m^{5/4}\left[1 + \dfrac{\log m}{\log P_n - 0.27}\right] \simeq m$	Almost yes
Lefroy and Davidson (1969)	$\dfrac{d_j}{P_n} = 1.06\dfrac{d_p}{P_n}$	$\dfrac{d_p}{d_p^o} = m^{1/4}$	No
Littman et al. (1979)	$\dfrac{d_j}{d_n} = \dfrac{2.1\exp(-0.018/A) + 1}{3.1}$ $\left[(0.862 + 0.219\left(\dfrac{P_n}{d_n}\right) - 0.053\left(\dfrac{P_n}{d_n}\right)\right]^2$ $A \equiv \dfrac{\rho_f}{\rho_p - \rho_f}\cdot\dfrac{u_t u_{mf}}{g d_n}$	$m\dfrac{2.1\exp(-0.018/A) + 1}{2.1\exp(-0.018/A^o) + 1}$ $= m$ if $\dfrac{\rho_f u_r d_p}{\mu} < 5.76$ $A = A^o$	Yes
Tanaka et al. (1980)	$\dfrac{d_j}{P_n} = \begin{cases} 0.8\left(\dfrac{\omega d_p}{P_n}\right)^{1/3}\left(\dfrac{u_0}{u_{mf}}\right)^{3/5}(\tan\phi_r)^{1/3} & (u_0/u_{mf} < 5) \\ 2.5\left(\dfrac{\omega d_p}{P_n}\right)^{1/3}(\tan\phi_r)^{1/3} & (u_0/u_{mf} > 5) \end{cases}$ $\omega \simeq 1$	$\begin{cases} \left(\dfrac{P_n}{P_n^o}\right)\left(\dfrac{d_p}{d_p^o}\cdot\dfrac{P_n^o}{P_n}\right)^{1/3}\left(\dfrac{u_0}{u_0^o}\cdot\dfrac{u_{mf}^o}{u_{mf}}\right)^{3/5} = m^{3/4} \\ \left(\dfrac{P_n}{P_n^o}\right)\left(\dfrac{d_p}{d_p^o}\cdot\dfrac{P_n^o}{P_n}\right)^{1/3} = m^{3/4} \end{cases} \simeq m$	Almost yes
Horio et al. (1980b)	$\dfrac{d_j}{d_n} = 1.56\left(\dfrac{f_j Fr_p}{\sqrt{k}\cdot\tan\phi_r}\right)^{0.3}\left(\dfrac{d_n}{P_n}\right)^{0.3}$ $Fr_p \equiv \dfrac{\rho_f u_n^2}{(1-\epsilon_{mf})\rho_p d_p g}$ $k \equiv \dfrac{1-\sin\phi_r}{1+\sin\phi_r}, f_j \simeq 0.02$	$\left(\dfrac{d_n}{d_n^o}\right)\left(\dfrac{f_j Fr_p\sqrt{k^o}\tan\phi_r^o}{f_j^o Fr_p^o\sqrt{k}\tan\phi_r}\right)^{0.3}$ $\cdot\left(\dfrac{d_n}{d_n^o}\dfrac{P_n^o}{P_n}\right)^{0.2} = m$	Yes

Table 3. Consistency of Previous Jet Height Correlations with Present Similarity Rule

Investigators	Correlation	h_j/h_j^o	Consistency
Basov et al. (1969)	$h_j' = \dfrac{1.26 d_p G^{0.35}}{7\times10^{-6} + 0.566 d_p}$ $h_j = h_j' - D_{b0}'$	$\dfrac{h_j'}{h_j^o} = m^{7/32}\dfrac{7\times10^{-6} + 0.566 d_p^o}{7\times10^{-6} + 0.566 d_p^o m^{1/4}}$	No
Merry (1975)	$\dfrac{h_j}{d_n} = 5.2\left(\dfrac{\rho_f d_n}{\rho_p d_p}\right)^{0.3}\left[1.3\left(\dfrac{u_n^2}{g d_n}\right)^{0.2} - 1\right]$	$m^{1.225}\dfrac{1.3m^{0.15}(u_n^{o2}/g d_n^o) - 1}{1.3(u_n^o/g d_n^o) - 1} = m^{1.35}$	Almost yes
Toei et al. (1974)	$h_j = 0.6G^{1/3}$	$\left[\dfrac{A_t(u_0 - u_{mf})}{A_t^o(u_0^o - u_{mf}^o)}\right]^{1/3} = m^{5/6}$	Almost yes
Yang and Keairns (1979)	$\dfrac{h_j}{d_n} = 15\,Fr_n'^{0.187}, Fr_n \equiv \dfrac{\rho_f u_n^2}{(\rho_p - \rho_f)g d_n}$	$\left(\dfrac{u_n}{u_n^o}\right)^{0.374}\left(\dfrac{d_n}{d_n^o}\right)^{0.813} = m$	Yes
Tanaka et al. (1980)	$h_j = \begin{cases} 0.6G^{0.4} & (u_0/u_{mf} > 7) \\ 0.31\omega P_n\left(\dfrac{P_n\tan^2\phi_r}{\omega d_p}\right)^{1/3} & (\omega \simeq 1)\quad (u_0/u_{mf} < 5) \end{cases}$	$\left[\dfrac{A_t(u_0 - u_{mf})}{A_t^o(u_0^o - u_{mf}^o)}\right]^{0.4} = m \quad (u_0/u_{mf} > 7)$ $\left(\dfrac{P_n^4 d_p^o}{P_n^{o4} d_p}\right)^{1/3} = m^{5/4} \quad (u_0/u_{mf} < 5)$	Yes to almost yes
Horio et al. (1980b)	$\dfrac{h_j}{P_n} = \dfrac{0.857}{\sqrt{k}}[1.2(d_j/P_n)^{-0.095} - 1]\ln\left(\dfrac{2u_{mf}}{u_0}\right)$ $\delta u_0 = \begin{cases} 0.004\text{m/s} & (d_p > 0.1\text{mm}) \\ 0.05u_{mf} & (d_p < 0.1\text{mm}) \end{cases}$ $k = (1-\sin\phi_r)/(1+\sin\phi_r)$	$m\dfrac{\ln\left(\dfrac{2u_{mf}}{\delta u_0}\right)}{\ln\left(\dfrac{2u_{mf}^o}{\delta u_0^o}\right)} = \begin{cases} m\left[1 + \dfrac{5.5 + \ln\sqrt{m}}{5.5 + \ln(2u_{mf})}\right] & (d_p > 0.1\text{mm}) \\ m & (d_p < 0.1\text{mm}) \end{cases}$	Almost yes to Yes

Table 4. Properties of Particles

Particle	Material	d_p μm	u_{mf} (observed) m/s	u_{mf} (Wen-Yu, 1966) m/s
GB376	Glass beads	376	0.112	0.112
GB305	Glass beads	305	0.074	0.075
GB236	Glass beads	236	0.046	0.045

same column under the same $u_0 - u_{mf}$. The experimental conditions are given in Table 7.

In series B and C the ratio of the cloud radius to the bubble radius was supposed to change run by run. In the series B conditions α_b, defined by Eq. 26, changes $\sqrt{m}$ times since $u_{b\infty}$ changes $\sqrt{m}$ times with a scale change of m times while u_{mf} remains constant. In series C, α_b varies 2.42 times from run IV to run V due to the change in u_{mf}. This change in α_b affects the smaller bubbles more than it affects the larger ones because in the case of larger bubbles the cloud becomes relatively thinner and the effect of the difference in cloud diameter becomes negligible.

Measuring techniques for bubbles

All bubbling data were obtained by analysis of a video record of bubble bursts at the bed surface. Motion pictures were taken by a video camera (SONY rotary shutter camera RSC 1110N, shutter speed 1/500, 60 frames per second). From the pictures reproduced on the TV screen the outlines of the bursting bubble bulge were duplicated on tracing paper. Then the two-dimensional data from the paper with regard to the location of each bubble center and the bubble radius were fed to a computer (FACOM M200) through a digitizer. The bubble diameter was determined from the diameter of the bursting bubble bulge according to the Tanimoto et al. (1983) correlation.

The average bubble diameter at a given height was calculated as the volume-averaged diameter of the bubbles that passed the corresponding cross section. About 100 bubble samples in a series were taken for each cross section.

Calculation of radial distribution of superficial bubble velocity

To determine a superficial bubble velocity distribution from video pictures is necessary to take into account the finite volumetric effect of bubble passage around the trajectory of the bubble center. In this data-processing algorithm the bubble shape was approximated by a cylindrical rod of the height $\bar{l}_b$, as shown in Figure 3a, to avoid too many complexities. The local superficial bubble velocity is given as the following summation of bubble height divided by the elapsed time:

$$u_b\epsilon_b = \left[\sum_j \bar{l}_{b,j}\right] \Big/ t. \tag{57}$$

As can be seen in Figure 3b the column radius was divided into 100 sections and the circumference of each section was divided into 60 sections. Thus, including the column center, a total of 101 nodes were defined. Once the $u_b\epsilon_b$ values for all the nodes were calculated, an average was obtained for the whole points on each circumference. This yielded the radial distribution of $u_b\epsilon_b$.

Table 5. Experimental Conditions for Test Series A

	Run I (base condition)	II	III
D_t, m	0.24	0.10	0.041
m	1.00	0.417	0.171
$m^{1/2}$	1.00	0.645	0.413
Particles	GB376	GB305	GB236
u_{mf}, m/s	0.112	0.074	0.046
u_{mf}/u^o_{mf}	1.00	0.661	0.411
u_0, m/s	0.224	0.146	0.092
$u_0 - u_{mf}$, m/s	0.112	0.072	0.046
$\frac{u_0 - u_{mf}}{(u_0 - u_{mf})^o}$	1.00	0.643	0.411

Table 6. Experimental Conditions for Test Series B

	Run I (base condition)	IV	VI
D_t, m	0.24	0.10	0.041
m	1.00	0.417	0.171
$m^{1/2}$	1.00	0.645	0.413
Particles	GB376	GB376	GB376
u_{mf}, m/s	0.112	0.112	0.112
u_0, m/s	0.224	0.184	0.158
$u_0 - u_{mf}$, m/s	0.112	0.072	0.046
$\frac{u_0 - u_{mf}}{(u_0 - u_{mf})^o}$	1.00	0.643	0.411

Results

Bubble size distributions

Longitudinal distributions of cross-sectional average bubble diameter are shown in Figure 4 with those predicted by correlations of the Mori and Wen (1975), Rowe (1976), and Darton et al. (1977). As expected from the theory, the results from all the series fall into the same distribution within the range of experimental error.

Not only the cross-sectional averages, but also the bubble size distribution around the average at each dimensionless height coincide. Figure 5 shows that the cumulative distribution of the bubble diameter at each height in each run coincides with that of the base condition for the corresponding height. This implies

Table 7. Experimental Conditions for Test Series C

	Run IV	II	V
D_t, m	0.10	0.10	0.10
Particles	GB376	GB305	GB236
u_{mf}, m/s	0.112	0.074	0.046
u_0, m/s	0.184	0.146	0.118
$u_0 - u_{mf}$, m/s	0.072	0.072	0.072

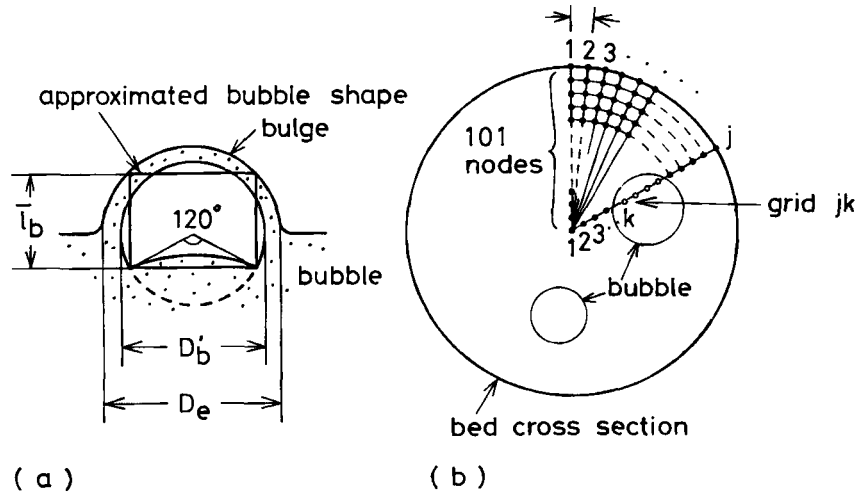

Figure 3. Method for $u_b\epsilon_b$ calculation.
(a) approximated bubble shape. (b) grid for sampling.

that the bubble growth process is insensitive to the cloud size differences, as has already been assumed in the previous bubble size correlations and coalescence models.

Radial bubble flow distribution

In Figure 6 the changes in the radial distributions of superficial bubble velocity $u_b\epsilon_b$ with dimensionless height are shown for the three experimental series. For series A and B the radial distributions at each height agree within the range of experimental error, although the discrepancies are slightly larger for the cases of $L_{mf}/D_t = 0.6$ and 0.8 in series A. In series C the curves for run V change from a circumferential flow at the bottom to a central flow at the top. However, from the present data the cause of this is uncertain. Like the bubble size distributions, the radial bubble flow rate seems to be insensitive to the difference in the hydrodynamics of gas in the emulsion phase as far as the group B particles of the Geldart (1973) classification are concerned.

Change in time scale

Figures 7 and 8 show the experimental results for the change in bubble frequency at a given L_{mf}/D_t due to the change in the bed scale for series A and B, respectively. Figure 9 shows the longitudinal distribution of bubble frequency for the series C runs. The good agreement between the bubble frequencies from the three runs shows that when the column is not changed, the bubbling characteristics become similar for the same $u_0 - u_{mf}$. This result is probably restricted to the group B particles. When the column diameter was changed according to the present similarity rule the frequency decreased in proportion with $\sqrt{D_t}$ (Figures 7 and 8).

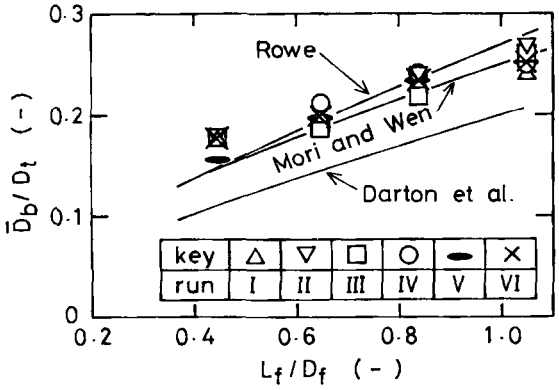

Figure 4. Longitudinal distribution of cross-sectional average bubble diameter.

The above result, however, is completely consistent with the present theory. In the scale change by the present rule the scale of length divided by time only varies $\sqrt{m}$ times when the length scale is changed m times. This means that the time scale is also changed $\sqrt{m}$ times. Accordingly, bubble frequency changes $1/\sqrt{m}$ times. In other words, if the present rule is applied for the scale-down from a commercial concept to a smaller unit, the phenomena in the smaller unit progress $\sqrt{m}$ times faster than those in the commercial unit. Therefore, if we can adjust any rate phenomena such as reactions and heat transfer so that their rates change $\sqrt{m}$ times with the scale-up of m times, the whole system can be kept similar—although it is not always possible, as discussed in the following section.

Possibility of Similarities in Mass Transfer and Reaction

Although the present similarity rule is restricted within the similarity of hydrodynamic conditions, it is interesting to study how much the rule can be extended to the phenomena containing other rate processes, such as mass transfer and chemical reaction. In the case of mass transfer between the bubble and cloud phases, both gas convection and diffusion contribute to the overall rate. Following Davidson and Harrison (1963) we can write

$$K_{BC} = 4.5\frac{u_{mf}}{D_b} + 5.85\frac{D^{*0.5}g^{0.25}}{D_b^{1.25}}. \qquad (58)$$

It may be worth noting here that this correlation is also valid for a slow bubble for which the cloud boundary is not closed. The first term in the above correlation represents the convection and

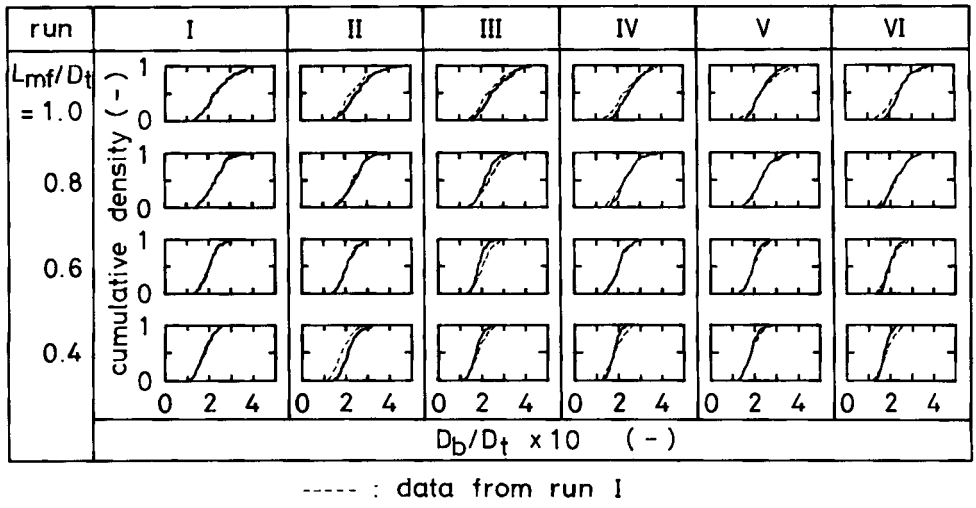

Figure 5. Cumulative distribution of bubble diameter at different heights.

the second represents the diffusion. Taking the ratio of the latter to the former and dropping the numerical constant, which is roughly unity, we have

$$\beta \equiv \frac{D^{*0.5} g^{0.25}}{u_{mf} D_b^{0.25}} \tag{59}$$

as a parameter to express the relative intensity of the diffusion compared to the convection. If β is much greater than unity the hydrodynamics have only a negligible effect on the gas interchange rate. If β is much smaller than unity the gas interchange is controlled by the hydrodynamics. In the reaction model the effect of gas interchange is expressed by a dimensionless parameter N_{BC} defined by

$$N_{BC} \equiv \frac{K_{BC} \epsilon_b L_f}{u_0}. \tag{60}$$

If the first term of the righthand side of Eq. 58 is expressed by K^o_{BC} and the corresponding N_{BC} by N_{BC0} becomes

$$N_{BC0} \equiv \frac{K^o_{BC} \epsilon_b L_f}{u_0} = \frac{4.5\, u_{mf}(u_0 - u_{mf}) L_f}{u_0 u_b D_b}. \tag{61}$$

In the situation of $\beta \ll 1$ the gas interchange is kept similar through the scale change because the invariance of $N_{BC} \simeq N_{BC0}$ is guaranteed by the present similarity rule. It can be seen from Figure 10 that the existing fluidized processes vary widely from the hydrodynamics control range to the diffusion dominating range. Those processes with fine catalysts belong to the range of $\beta > 10$, while fluidized bed combustors belong to the range of $\beta < 0.1$.

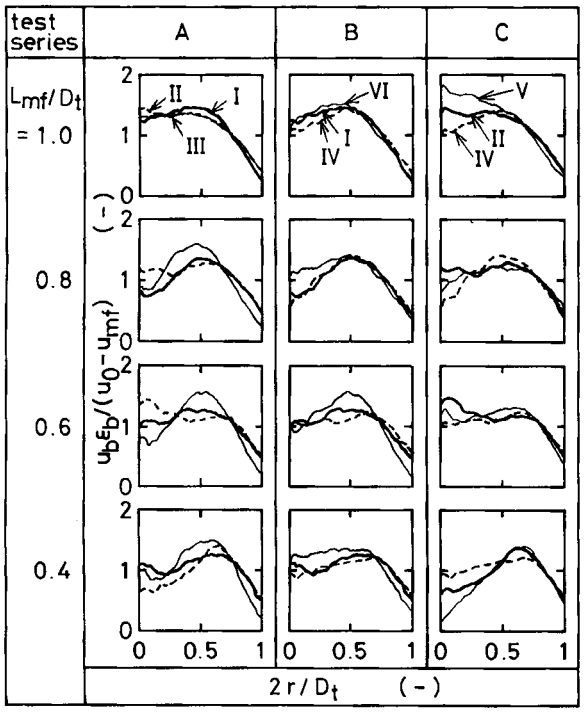

Figure 6. Radial distribution of superficial bubble velocity $u_b \epsilon_b$.

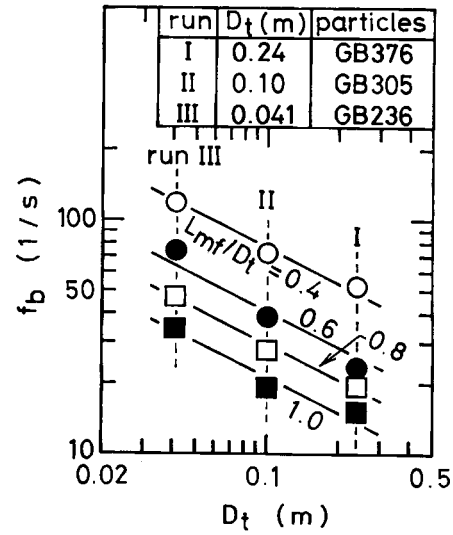

Figure 7. Bubble frequency in series A runs.

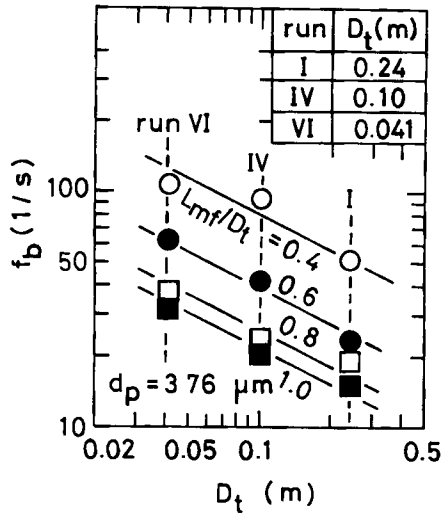

Figure 8. Bubble frequency in series B runs.

To attain a similarity in the chemical conversion, not only the mass transfer but also the reaction itself must be similar. From the consideration made in the preceding section, the $\sqrt{m}$ times change in the reaction rate is consistent with the $1/m$ times scale change under the present similarity rule. Computation was done to compare the overall conversions for commercial or pilot scale plants and for those of $1/m$ scale. The model used for the present computation was the three-phase bubble assemblage model (Horio and Nonaka, 1984). The model is similar to the three-phase bubble assemblage model of Peters et al. (1982). However, the gas downflow in the emulsion phase was neglected and only the conversions in the bubbling zone were computed. Figure 11 shows the result for a 500 MW atmospheric fluidized bed combustor (AFBC). If the same particles are used for beds of different scale, the broken lines are obtained. In Figure 11 the abscissa represents the dimensionless reaction rate constant N_r, which is defined by

$$N_r \equiv \frac{k_r L_{mf}}{u_0}, \tag{62}$$

where k_r is the apparent reaction rate constant for a first-order reaction. According to the rule of time-scale change k_r is

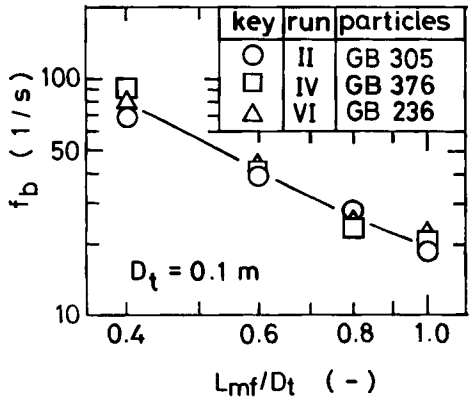

Figure 9. Longitudinal distribution of bubble frequency in series C runs.

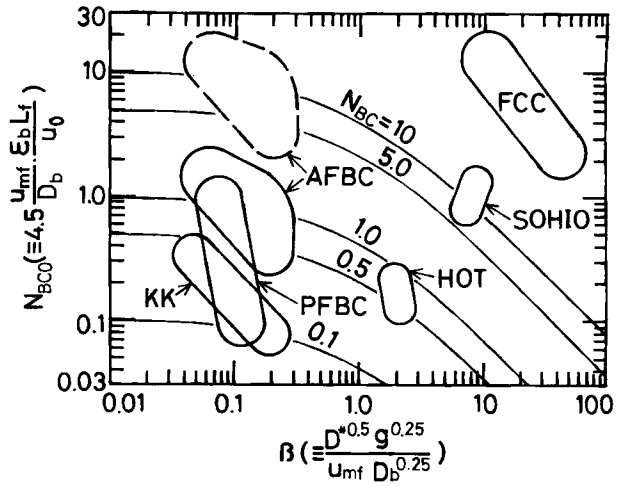

Figure 10. Operating range of various processes.

AFBC (atmospheric fluidized bed combustion): 20 t(steam)/h (Wakamatsu plant) ~1,640 t/h (500 MW conceptual design) (Tamanuki et al., 1979, 1981).
—— effect of internals not considered.
--- max. bubble dia. = pitch of heat transfer tube.
FCC (fluid catalytic cracking): 5,600 bbl/d (Yamaguchi, 1960).
HOT (heavy oil treating process): 250 BPSD, D_t = 1.6 m, L_f = 10 m (Kashiwara et al., 1982).
KK (Kunii-Kunugi thermal cracking process): 120 t/d, D_t = 1.6 and 2.7 m, L_f = 5.5 m (Kashiwara et al., 1982).
PFBC (pressurized fluidized bed combustion): Grimethope plant, A_t = 2 × 2 m^2, L_f = 4 m (Carls et al., 1980); Leatherhead plant, A_t = 1.2 × 0.6 m^2, L_f = 2.8 m (Hoy and Roberts, 1980).
SOHIO (SOHIO, Cat-21 acrylonitrile process): 230~470 t/d, D_t = 3.4 m, L_{mf} = 6.7 m (Ikeda, 1977).

changed to $1/\sqrt{m}$ times with the $1/m$ times change in the length scale. It is obvious that if the present similarity rule is completely satisfied, improved chemical similarity is obtained. However, in the high conversion range deviation from the $m = 1$ curve is evident. If the scale is decreased according to the present rule, the intensity of convection is decreased. The intensity of diffusion, however, remains constant. Therefore, the conversion is increased with the reduction in the plant size. The faster the reaction rate is, the more exaggerated this tendency is.

Since the apparent reaction rate constant k_r includes the

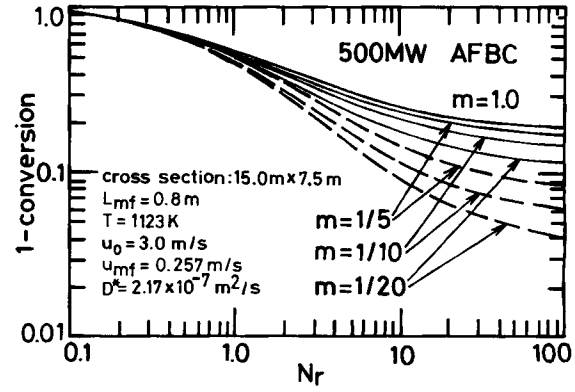

Figure 11. Test of chemical similarity for fluidized bed combustion.

—— both Eq. 41 and 42 are satisfied.
--- only Eq. 41 is satisfied.

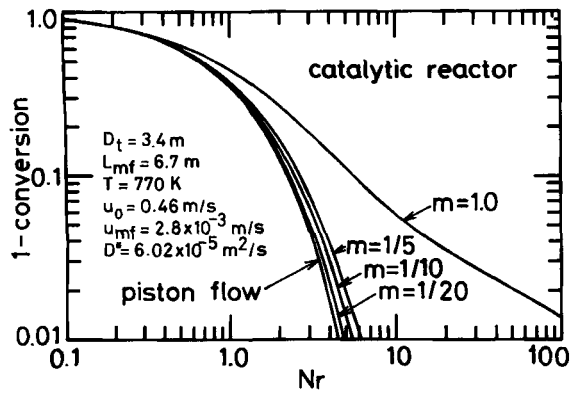

Figure 12. Test of chemical similarity for fluidized bed catalytic cracking.

effect of char holdup in the bed, we can write

$$k_r = \frac{6k_c X_c \rho_p (1 - \epsilon_{mf})}{d_c \rho_c}, \tag{63}$$

where k_c is the overall combustion rate constant and X_c is the char holdup. In fluidized bed combustion (FBC) the char holdup in the bed is about 1% and the reaction rate constant is approximately estimated assuming that the Sherwood number equals 2 and that the mass transfer is the rate-controlling step. Assuming that the average char particle size in the bed is 0.5×10^{-3} m, we have $N_r \simeq 10$. This indicates that the apparent reaction rate is adjusted in FBC so that the stoichiometric amount of oxygen is completely converted. Since the excess air ratio is about 0.2 in the ordinary AFBC condition, the necessary conversion for complete combustion of coal is 0.83. Although the maximum conversion for the case of $m = 1$ is still less than this value, probably because the effect of the in-bed heat transfer tubes was neglected, it can be seen that the 10-times scale-up or one-tenth scale-down can be done within 10% accuracy of the conversion. This suggests the possibility of applying the present similarity rule to a hot combustion experiment to study the effects of internals, distributor, and fuel feeder designs.

An example of computation for a catalytic reactor is shown in Figure 12. In the computation bubble splitting is also taken into account based on the Horio and Nonaka (1984) correlation. Because of the small bubble diameter, even the curve for $m = 1$ is fairly close to that of the plug flow. Nevertheless, the difference between the curves, not their closeness, should be stressed because it indicates that the contribution of bubble hydrodynamics cannot be neglected. However, even the one-fifth scale-down according to the present similarity rule brings about a result very close to the plug flow condition due to the sharp increase in the relative intensity of diffusion. Therefore, in the case of catalytic reactions with fine catalyst particles, it would be very difficult to predict the exact reaction performance of a commercial-scale plant directly from a small-scale experiment.

Concluding Remarks

Bubbling, jetting, and interstitial flow in a fluidized bed can be made geometrically similar with those in the beds of different scales if the column structure is similar and if the conditions of Eqs. 41 and 42 are satisfied. Theoretical derivation, test of consistency with the previous empirical correlations for bubble diameter and jet shape, experimental validation for group B particles, and examination of the possibility of extending the present rule into other rate phenomena have been presented. Thus, the possibility of applying the present similarity rule with the conventional identity rule has been confirmed. Further study is needed regarding:

1. Experimental testing of the present rule for group A particles
2. Applicability of the rule for controlling particle behavior
3. The possibility of extending the rule into the freeboard problem
4. Methodology for applying the present similarity rule to fluidized bed design and development.

Notation

A_t = bed cross-sectional area, m^2
B = set of all bubbles in the bed
B_i' = set of bubbles absorbed by bubble i
b = parameter, Eq. 15
d_c = char particle diameter, m
d_j = jet diameter, m
d_m = particle moving zone diameter around a distributor orifice, m
d_n = orifice diameter, m
d_p = surface volume mean particle diameter, m
D_b = bubble diameter, m
D_b' = diameter of bubble curvature, m
D_{b0} = initial bubble diameter, m
D_{bm} = maximum bubble diameter from total coalescence of bubbles, m
D_c' = diameter of cloud curvature, m
D_e = bubble eruption diameter, m
D_w = radial diffusivity of bed particles, m^2/s
D_t = column diameter, m
D_t' = thickness of two-dimensional bed, m
D^* = molecular diffusivity, m^2/s
e_z = unit z vector, e
f_b = bubble frequency per total bed cross section, 1/s
f_d = ratio of drift particle volume to bubble volume
f_i^* = splitting frequency of a single bubble, 1/s
f_w = wake fraction
F_{ij} = factor representing interaction between bubbles i and j
Fr = Froude number
g = gravity acceleration, m/s^2
$G = (u_0 - u_{mf})A_t/n$, bubble flow rate through an orifice, m^3/s
h_j = jet height, m
h_s = dead zone height, m
$k_b = u_b/\sqrt{gD_b}$, bubble velocity coefficient
$k_{b\infty}$ = velocity coefficient of a bubble in isolation
k_c = overall combustion rate constant, m/s
k_r = reaction rate constant, 1/s
K_{BC} = gas interchange coefficient between bubble and cloud phase, 1/s
K_{BC0} = gas interchange coefficient for negligible diffusion, 1/s
l_b = vertical length of bubble and probe intercept, m
l_j = jet length, m
L_f = fluidized bed height, m
L_{mf} = bed height at minimum fluidizing condition, m
m = magnification of length scale
n_n = number of orifices on the distributor
N_{BC} = dimensionless gas interchange coefficient
N_{BC0} = dimensionless gas interchange coefficient for negligible diffusion
N_r = dimensionless reaction rate constant
Pe_s = Peclet number for radial solid dispersion
P_n = orifice pitch, m
q_s = volumetric solid circulation rate, m^3 (emulsion)/s
r = radius, m
r_p = radial position of maximum bubble flow, m
R_b = bubble radius, m

R'_b = radius of bubble curvature, m
R_c = cloud radius, m
$R_t = D_t/2$, m
t = time, s
u_0 = superficial gas velocity, m/s
u_b = bubble rising velocity, m/s
$u_{b0} = u_b\epsilon_b$, local superficial bubble velocity, m/s
u_{bi} = rising velocity of bubble i, m/s
$u_{b\infty}$ = rising velocity of a bubble in isolation, m/s
u_e = interstitial gas velocity, m/s
u_{emf} = interstitial gas velocity at minimum fluidization, m/s
u_{mf} = minimum fluidization velocity, m/s
u_n = gas velocity at the outlet of an orifice, m/s
u_r = radial gas velocity around a bubble, m/s
u_s = slug rising velocity, m/s
u_t = terminal velocity, m/s
u_θ = θ direction gas velocity around a bubble, m/s
$\boldsymbol{v}$ = particle velocity vector, m/s
v_r = radial velocity of solid around a bubble, m/s
v_θ = θ direction velocity of solid around a bubble, m/s
x = horizontal coordinate, m
$x_{bi} = (x_{bi}, y_{bi}, z_{bi})$, location of bubble i, m
x_{0i} = initial location of bubble, i, m
X_c = mass fraction of char in the bed
y = horizontal coordinate, m
z = height above distributor, m
z_{b0} = height of initial bubble formation, m

Greek letters

$\alpha_b = u_{b\infty}/u_{emf}$
$\beta = D^{*0.5}\, g^{0.25}/u_{mf} D_b^{0.25}$, relative intensity of diffusion
Δu_{ij} = increment of velocity of bubble i by the presence of bubble j, m/s
ϵ_b = bubble fraction
ϵ_{mf} = void fraction of bed at minimum fluidization
θ = angle, rad
μ = viscosity, Pa · s
ν_t = turbulent kinematic viscosity of solids, m^2/s
ξ = parameter, Eq. 9
ϕ_r = angle of repose, rad
Φ_s^+ = dimensionless velocity potential of particles
Ψ_f^+ = dimensionless stream function of gas
ρ_c = density of char, kg/m^3
ρ_f = gas density, kg/m^3
ρ_p = particle density, kg/m^3

Superscripts

$+$ = dimensionless
o = original scale plant

Literature Cited

Anderson, T. B., and R. Jackson, "A Fluid Mechanical Description of Fluidized Beds," *Ind. Eng. Chem. Fundam.*, **6**, 527 (1967).

Baeyens, J., and D. Geldart, "An Investigation into Slugging Fluidized Beds," *Chem. Eng. Sci.*, **29**, 255 (1974).

Basov, V. A., et al., "Investigation of the Structure of a Nonuniform Fluidized Bed," *Int. Chem. Eng.*, **9**, 263 (1969).

Broadhurst, T. E., and H. A. Becker, "Onset of Fluidization and Slugging in Beds of Uniform Particles," *AIChE J.*, **21**, 238 (1975).

Carls, E. L., et al., "The IEA Grimethope Pressurized Fluidized Bed Combustion Experimental Facility," *Proc. 6th Int. Conf. Fluidized Bed Combust.*, **2**, 225 (1980).

Chiba, T., K. Terashima, and H. Kobayashi, "Bubble Growth in Gas Fluidized Beds," *J. Chem. Eng. Japan*, **6**, 78 (1973).

Clift, R., and J. R. Grace, "Coalescence of Bubbles in Fluidized Beds," *AIChE Symp. Ser.*, No. 116, **67**, 23 (1971).

Darton, R. C., et al., "Bubble Growth Due to Coalescence in Fluidized Beds," *Trans. Inst. Chem. Eng.*, **55**, 274 (1977).

Davidson, J. F., "Symposium on Fluidization—Discussion," *Trans. Inst. Chem. Eng.*, **39**, 223 (1961).

Davidson, J. F., and D. Harrison, *Fluidized Particles*, Cambridge Univ. Press, London, 50 (1963).

Fitzgerald, T., et al., "Testing of Cold Scaled Bed Modeling for Fluidized Bed Combustors," *Proc. 7th Int. Conf. Fludized Bed Combust.*, DOE/METC, **2**, 766 (1983).

———, "Testing of Cold Scaled Bed Modeling for Fluidized Bed Combustors," *Powder Technol.*, **38**, 107 (1984).

Fryer, C., "Fluidized Bed Reactors—Behavior and Design," Ph. D. Thesis, Monash Univ., Australia (1974).

Garg, S. K., and J. W. Pritchett, "Dynamics of Gas-Fluidized Beds," *J. Appl. Phys.*, **46**, 4,493 (1975).

Geldart, D., "The Size and Frequency of Bubbles in Two- and Three-Dimensional Gas-Fluidized Beds," *Powder Technol.*, **4**, 41 (1971).

———, "Types of Gas Fluidization," *Powder Technol.*, **7**, 285 (1973).

GOLFERS, "Behavior of a 1 m Square Gas-Fluidized Bed," *Kagaku Kogaku Ronbunshu*, **8**, 464 (1982).

Hirama, T., M. Ishida, and T. Shirai, "The Lateral Dispersion of Solid Particles in Fluidized Beds," *Kagaku Kogaku Ronbunshu*, **1**, 272 (1975).

Horio, M., H. Kiyota and I. Muchi, "Particle Movement on a Perforated Plate Distributor of Fluidized Bed," *J. Chem. Eng. Japan*, **13**, 137 (1980a).

Horio, M., T. Yamada, and I. Muchi, "Prediction of Vertical Jet Shape in Fluidized Beds and Spouted Beds," Preprint, 14th Fall Meet. Soc. Chem. Eng. Japan, SB317 (1980b).

Horio, M., Y. Sawa, and I. Muchi, "Similarity Rule and Scale-up of Fluidized Beds," Preprint, 16th Fall Meet. Soc. Chem. Eng. Japan, SD301 (1982).

Horio, M., J. Liu, and I. Muchi, "Direct Simulation for Predicting Bubble Distribution and Particle Circulation Pattern in Large-Scale Fluidized Beds," *Kagaku Kogaku Ronbunshu*, **9**, 176 (1983a).

Horio, M., et al., "Horizontal Jet Penetration into Powder Beds under Different Aeration Conditions," *Kagaku Kogaku Ronbunshu*, **9**, 609 (1983b).

Horio, M., and A. Nonaka, "A Generalized Bubble Diameter Correlation and Its Application to Fluidized Bed Reactor Modeling," Ms. No. 1471, AIChE Ann. Meet., San Francisco (1984).

Hoy, H. R., and A. G. Roberts, "Investigations on the Leatherhead Pressurized Facility," *Proc. 6th Int. Conf. Fluidized Bed Combust.*, **2**, 241 (1980).

Ikeda, Y., "Fluidized-Bed Reactions in Petrochemical Processes—Sohio Acrylonitrile Process," *J. Japan Petrol. Inst.*, **20**, 619 (1977).

Jahnig, C. E., D. L. Champbell, and H. Z. Martin, "History of Fluidized Solids Development at EXXON," *Fluidization*, Grace and Matsen, eds., Plenum, New York, 3 (1980).

Kashiwara, H., et al., eds., *Heavy Oil Processing Handbook*, Chemical Daily Co., Ltd., (1982).

Kuhn, T. S., *The Structure of Scientific Revolutions*, Univ. Chicago Press (1962).

Kunii, D., and O. Levenspiel, "Bubbling Bed Model for Kinetic Processes in Fluidized Beds," *J. Chem. Eng. Japan*, **2**, 122 (1969).

Lanneau, K. P., "Gas-Solids Contacting in Fluidized Beds," *Trans. Inst. Chem. Eng.*, **38**, 125 (1960).

Lefroy, G. A., and J. F. Davidson, "The Mechanics of Spouted Beds," *Trans. Inst. Chem. Eng.*, **47**, 120 (1969).

Lewis, W. K., and E. R. Gilliland, U. S. Patent No. 2,498,088 (Feb. 21, 1950; original application, Jan. 3, 1940).

Littman, H., et al., "Prediction of the Maximum Spoutable Height and the Average Spout-to-Inlet Tube Diameter Ratio in Spouted Beds of Spherical Particles," *Can. J. Chem. Eng.*, **57**, 684 (1979).

Malek, M. A., L. A. Madonna, and B. C. Y. Lu, "Estimation of Spout Diameter in a Spouted Bed," *IEC Proc. Des. Dev.*, **2**, 30 (1963).

Merry, J. M. D., "Penetration of Vertical Jets into Fluidized Beds," *AIChE J.*, **21**, 507 (1975).

Miyauchi, T., et al., "Transport Phenomena and Reaction in Fluidized Catalyst Beds," *Adv. in Chem. Eng.*, **11**, 275 (1981).

Mori, S., and C. Y. Wen, "Estimation of Bubble Diameter in Gaseous Fluidized Beds," *AIChE J.*, **21**, 109 (1975).

Murray, J. D., "On the Mathematics of Fluidization. 2: Steady Motion of Fully Developed Bubbles," *J. Fluid Mech.*, **22**, 57 (1965).

Nguyen, X. T., L. S. Leung, and R. H. Weiland, "Measurement of Through-Flow Velocities in a Bubble in Two-Dimensional Fluidized Beds," *Fluidization Technology*, D. L. Keairns, ed., Hemisphere, Washington, DC, **1**, 297 (1976).

Peters, M. H., L. S. Fan, and T. L. Sweeney, "Reactant Dynamics in Catalytic Fluidized Bed Reactors with Flow Reversal of Gas in the Emulsion Phase," *Chem. Eng. Sci.*, **37**, 553 (1982).

Reh, L., "Fluidized Bed Processing," *Chem. Eng. Prog.*, **67**(2), 58 (1971).
Rowe, P. N., et al., "Bubbles in Fluidized Beds," *Nature* (London), **195**, 278 (1962).
Rowe, P. N., B. A. Partridge and E. Lyall, "Cloud Formation around Bubbles in Gas-Fluidized Beds," *Chem. Eng. Sci.*, **19**, 973 (1964).
Rowe, P. N., "Prediction of Bubble Size in a Gas-Fluidized Bed," *Trans. Inst. Chem. Eng.*, **54**, 285 (1976).
Stewart, P. S. B., and J. F. Davidson, "Slug Flow in Fluidized Beds," *Powder Technol.*, **1**, 61 (1967).
Tamanuki, S., "Development of Power Generation Technology via Fluidized Bed Combustion," Preprint, 1st Meet. Coal Utilization Tech., Coal Mining Res. Center, Japan, 1 (1979).
Tamanuki, S., H. Katayama and N. Takami, "The 20 t/h Fluidized Bed Boiler Pilot Plant Test," Preprint, 3rd Meet. Coal Utilization Tech., Coal Mining Res. Center, Japan, 65 (1981).
See also Terada, H., et al., "Current Topics on Testing of the 20 t/h fluidized Bed Boiler," *Proc. 7th Int. Conf. Fluidized Bed Combust.*, 876 (1982).
Tanaka, I., et al., "Perforated Plate Distributor of Fluidized Beds—Diameter and Height of Spout above Distributor," *J. Soc. Powder Tech. Japan*, **17**, 22 (1980).
Tanimoto, H., et al., "Mechanism of Particle Ejection from Gas-Fluidized beds," *Kagaku-Kogaku-Ronbunshu*, **9**, 497 (1983).
Toei, R., et al., "Deformations and Splittings of a Bubble in a Two-Dimensional Fluidized Bed—Experimental Results," *J. Chem. Eng. Japan*, **7**, 447 (1974).
Toomey, R. D., and H. F. Johnstone, "Gaseous Fluidization of Solid Particles," *Chem. Eng. Progr.*, **48**, 220 (1952).
Wen, C. Y., and Y. H. Yu, "Mechanics of Fluidization," *AIChE Symp. Ser.*, No. 62, **62**, 100 (1966).
Werther, J., "The Influence of the Bed Diameter on the Hydrodynamics of Gas Fluidized Beds," AIChE Meet. Detroit (1973).
Whitehead, A. B., and A. D. Young, "Fluidization Performance in Large-Scale Equipment," *Proc. Int. Symp. Fluidization*, Eindhoven, Netherlands, 284 (1967).
Yagi, S., I. Muchi, and T. Aochi, "On the Conditions of Fluidization of Bed," *Kagaku-Kikai*, **16**, 307 (1952).
Yamaguchi, T., "Investigation on Fluid Catalytic Cracking. I: About the Operating Factors," *J. Japan Petrol. Inst.*, **3**, 629 (1960).
Yang, W. C., and D. L. Keairns, "Estimating the Jet Penetration Depth of Multiple Vertical Grid Jets," *Ind. Eng. Chem. Fundam.*, **18**, 317 (1979).
Yasui, J., and L. N. Johanson, "Characteristics of Gas Pockets in Fluidized Beds," *AIChE J.*, **4**, 445 (1958).
Yerushalmi, J., D. H. Turner, and A. M. Squires," The Fast Fluidized Bed," *IEC Proc. Des. Dev.*, **15**, 47 (1976).

Manuscript received Jan. 3, and revision received Aug. 23, 1985.